SYNTHESIS AND CHARACTERIZATION OF ALUMINA SUPPORTED HIGHLY DISPERSED AND HIGH LOADING MOLYBDENUM SULFIDE CATALYSTS VIA ION-EXCHANGE METHOD

BY

NOKTAN MOHAMMED NOKTAN ALYAMI

A Thesis Presented to the
DEANSHIP OF GRADUATE STUDIES

KING FAHD UNIVERSITY OF PETROLEUM & MINERALS
DHAHRAN, SAUDI ARABIA

In Partial Fulfillment of the
Requirements for the Degree of

MASTER OF SCIENCE

In

CHEMISTRY

MAY 2013

KING FAHD UNIVERSITY OF PETROLEUM & MINERALS
DHAHRAN- 31261, SAUDI ARABIA
DEANSHIP OF GRADUATE STUDIES

This thesis, written by **Noktan Mohammed Noktan AlYami** under the direction of his thesis advisor and approved by his thesis committee, has been presented and accepted by the Dean of Graduate Studies, in partial fulfillment of the requirements for the degree of **Master of Science in Chemistry.**

Dr. Mohammed A. AlDaous
(Advisor)

Dr. Abdullah J. AlHamdan
Department Chairman

Dr. Khalid A. AlMajnouni
(Member)

Dr. Salam A. Zummo
Dean of Graduate Studies

Dr. Mohammed A. Morsy
(Member)

7/1/14
Date

Dedication

To my parents and loved ones

ACKNOWLEDGMENTS

I would like to express my gratefulness to my thesis advisor, Dr. Mohammed Abdulmajeed Al-Daous, for allowing me to work under his supervision, and for his continuous contribution to this work and also for his usual support to overcome so many obstacles through out my research with his patience and understanding.

Also, I would like to thank Dr. Mohammed Ali Morsy, Associate Professor, Department of Chemistry of King Fahd University of Petroleum and Minerals (KFUPM), and Dr. Khalid AlMajnoni, Lab Scientist of Saudi Aramco for their advices and encouragements to pursuing the work for the excellence. I would like to extend my gratitude to Dr. Husin Sitepu and the management of R&D Center of Saudi Aramco for their continuous encouragements and assistance to ease the way to get my MS degree.

To my parents, brothers and sisters, to my wife and our son (Muhammad), I say words alone cannot express my deep appreciation to you for your encouragement and prayers. I only pray Allah reward you abundantly. To all my friends especially Muneeb and Abdullah, I say a big thanks to you for your assistance and prayers.

I would also like to acknowledge King Abdulaziz City for Science and Technology (KACST) for the support provided through the Science and Technology Unit at King Fahd University of Petroleum and Minerals (KFUPM) for funding the work through project No. 10-PET1394-04 as part of the National Science, Technology and Innovation Plan.

TABLE OF CONTENTS

LIST OF TABLES

LIST OF FIGURES

LIST OF ABBREVIATIONS

-SA: Surface Area measured by BET.

-Vp: Pore volume measure @ $P/P_o = 0.994$

-Dp: Pore diameter measured using BJH method of the desorption branch.

-NA: Not Applicable.

-HDS: Hydrodesulphurization

--HYD: Hydrogenation

-PDDA: Poly(diallyldimethylammonium chloride)

-PSS: Poly(sodium 4-styrenesulfonate)

ABSTRACT

Full Name : [Noktan Mohammed Noktan AlYami]
Thesis Title : [Synthesis And Characterization of Alumina Supported Highly Dispersed and High Loading Molybdenum Sulfide Catalysts via Ion-Exchange Method]
Major Field : [Chemistry]
Date of Degree : [[May 2013]

Intensive sulfur reduction in gasoline and diesel oil is becoming more and more necessary due to the implementation of more stringent specifications in many countries. One of the approaches to desulfurization is catalytic hydrodesulfurization (HDS) which has proved to be very effective for reactive sulfur compounds. However, HDS of alkylated thiophene still presents difficulty when using conventional HDS catalysts. One way to overcome this difficulty is through development of supported Molybdenum Sulfide (MoS_2) catalyst with high loading and high dispersion.

In this study, proposed catalytic materials were synthesized and composed of MoS_2 catalysts promoted by Cobalt (Co) and supported onto polyelectrolyte-coated gamma-alumina (γ-Al_2O_3). The synthesis procedure involved the use of polyelectrolyte assisted ion-exchange formation of highly dispersed molybdate species onto the surface of the supports at different pH values including 4, 6 and 8 in order to afford 15-20 wt% Mo loading. Inductively coupled plasma (ICP) reveals that the prepared catalysts at pH equals to 8 and 4 were the best Mo loading with almost 6-16-wt%. In addition, the physicochemical properties of both precursor systems and their corresponding activated catalyst were verified by various analytical techniques. As suggested by the various characterization techniques, the catalysts with different Mo loading at different PH values show no sign of change in the Mo species structure. Subsequently, the Mo/Polyelectrolyte-coated γ-Al_2O_3 were impregnated by Co solutions with different concentration including (0.005, 0.01, 0.025, 0.05, 0.1, 0.15, 0.2) M and at specific pH= 5.5. All the synthesized catalysts were sulfided to afford the final product in the form of sulfide which is $CoMoS_2$/γ-Al_2O_3. Those catalysts were tested for HDS and HYD and show superior activity and stability in the overall hydrodesulfurization (HDS) reactions of 2-methylethiophene (2-MT) and less affinity towards the hydrogenation (HYD) reations of (2,3dimethylebut2ene) in comparison with the impregnated catalyst used as a reference.

ملخص الرسالة

الاسم الكامل: : نقطان بن محمد بن نقطان آل بحري اليامي

عنوان الرسالة: تحضير وتوصيف المحفز كبريتيد الموليبدينوم بمساعدة الألومينا المغطاة بـ البولي اليكتروليتي ودعم معدن الكوبلت بواسطة التبادل الأيوني

التخصص: الكيمياء

تاريخ الدرجة العلمية: مايو-2013

في هذا البحث، تم تصنيع المواد الحافزة المقترحة و تتكون من MoS$_2$ التي تحتوي على معدن الكوبالت (Co) كمدعم وايضاً على جاما الألومينا (γ-AL$_2$O$_3$) المغطاة بـ البولي الكتروليتي كمساعد. تشارك الإجراء التوليف استخدام البولي الكتروليتي ساعد تشكيل التبادل الأيوني الأنواع موليبدات فرقت غاية على سطح دعما عند قيم درجة الحموضة المختلفة بما في ذلك 4 و 6 و 8 من أجل تحمل 15-20 ٪ بالوزن مو بولي الكتروليتي التي تغ التحميل . البلازما بالحث (ICP) يكشف عن أن المواد الحفازة المعدة في درجة الحموضة يساوي 8 و 4 كانت أفضل مو التحميل مع ما يقرب من 6 -16- ٪ بالوزن . بالإضافة إلى ذلك، تم التحقق من الخصائص الفيزيائية لكلا النظامين السلائف و المقابلة حافزا على تفعيلها من خلال التقنيات التحليلية المختلفة. كما اقترح من قبل مختلف تقنيات توصيف و المحفزات مع مختلف مو التحميل في القيم PH مختلفة لا تظهر أي علامة على تغير في بنية الأنواع مو . في وقت لاحق ، تم مشربة مو / المغلفة متضاعف الكتروليتي AL2O3 - γ من قبل شركة الحلول مع تركيز مختلفة بما في ذلك (0.005 ، 0.01، 0.025 ، 0.05، 0.1، 0.15 ، 0.2) م و درجة الحموضة في محددة = 5.5. تم sulfided جميع المحفزات توليفها على تحمل المنتج النهائي في شكل كبريتيد وهو . CoMoS2/γ-Al2O3 تم اختبار تلك المحفزات ل HDS و HYD و تظهر النشاط متفوقة والاستقرار في السلفرة الهيدروجينية العام (HDS) ردود الفعل من 2 methylethiophene (2 -MT) و تقارب أقل تجاه الهدرجة reations (HYD) من (2،3 dimethylebut2ene)بالمقارنة مع المحفز مشربة استخدامها كمرجع

CHAPTER 1

INTRODUCTION

Elimination of sulfur-containing molecules from petroleum feedstock is necessary in order to meet the severe restriction son the sulfur concentrations in fuels [1,2]. One approach is to One approach is based on the improvement of current hydrodesulfurization (HDS) technology. Utilization of more active catalysts, because of their much lower investment costs, may be the most attractive solution for petroleum refineries. Despite some interesting results concerning the catalytic activity of new phases such as carbides [3] or phosphides [4], the classic sulfide-based formulations, composed of a molybdenum sulfide (MoS_2), or tungsten sulfide, phase promoted by cobalt or nickel and usually supported on alumina [5] appear to be the most promising in responding to the challenges. The emergence of much more active catalysts, such as NEBULA, jointly developed by Exxon Mobile, Azko Nobel, and Nippon Ketjen [6], or SMART, Chevron and Grace Davison [7], illustrates the fact that MoS_2-based materials, although have been around for about 70 years, still have a great potential.

In particular, one of the ways to improve MoS_2-based catalysts could be to increase the active phase loading. However, a high dispersion of active phase cannot be achieved in this case by sulfidation of conventional oxide precursors, and other approaches should be used to create small sulfide particles and to maintain their stability under HDS conditions [5]. The recently developed method in our laboratory of a polyelectrolyte assisted hydrothermal growth of up to 20 wt.% nano-molybdate particles from an aqueous solution on carbon, which upon sulfidation formed MoS_2 with high dispersion, is a potentially promising technique for use with oxide supports [8]. The role of the polyelectrolyte multilayer structure in this method is two-fold; first it provides a nucleation region for the precursor nano-molybdate particles [9], a process that has been reported to occur with polymer brush/multilayer nano-reactors through the confinement or immobilization of the precursor ions, thus preventing the formation of large agglomerated solid particles [10]. The second role of the polyelectrolyte multilayer is that carbonaceous materials formed through decomposition of the organic polymer during sulfidation of the catalyst precursor, which is well dispersed over the sulfide particles, may prevent MoS_2 slaps from sintering [11,12].

Supports play an important role in determining the nature and number of active sites, and consequently, in the activity of the catalysts. The proposed supports for this study is the conventionally used gamma–alumina (γ–Al_2O_3). Nevertheless, it was recognized in the very first studies related to CoMo or NiMo/Al_2O_3 catalysts that alumina is not an inert carrier and that the promoter ions, Co and Ni, can react with the support and occupy octahedral or tetrahedral sites in the external layers [13]. Also, when heptamolybdate is deposited on γ–Al_2O_3, Anderson-type heteropolymolybdate $[Al(OH)_6Mo_6O_{18}]$ has been found to form a very strong metal-support interaction that makes the sulfidation of the Mo difficult [14]. Hence, the carbonaceous material produced from the decomposition of the polyelectrolytes is expected in this case to reduce these interactions by acting as a thin layer at the interface between the alumina surface and the active phase [15].

1.1 Research Objectives

The following are the objectives of the proposed research:

a) To synthesize supported highly dispersed MoS_2 catalyst with active phase loading of 15-20 wt.% on macroporous γ–Al_2O_3.

b) To characterize the catalyst in order to ascertain the chemical form, the amount and the dispersion of the active ingredient both in the precursor material and in the activate phase.

c) To conduct hydrodesulfurization and hydrogenation reactions of synthetic model FCC gasoline on the synthesized catalysts with the aim of identifying the factors that can favor HDS and minimize olefin hydrogenation in model FCC gasoline.

CHAPTER 2

LITERATURE REVIEW

2.1 Introduction

In an attempt to meet the growing demand for ultra low sulfur fuel and satisfying the strict regulation of sulfur standards around the world, a number of new concepts and technologies have been developed in the last 20 years in addition to the choice of revamping the conventional hydrotreaters. It has been reported that most of the hydrotreaters that were installed to meet the 1993 low sulfur requirement (500 ppm) can be revamped for ultra low sulfur diesel (10 ppm) production with reasonable increase in operational and capital costs [16]. Though several options such as increasing the severity of operating conditions, increase catalyst volume, removal of H2S from recycle gas, improve feed distribution in the reactor by using high efficiency vapor/liquid distribution trays, and use of easier feeds have been explored [17], the use of highly active catalysts is still of importance. The use of improved hydrotreating catalysts with high activity can improve considerably the desulfurization performance of existing hydrotreating units.

New improved catalysts have been developed by major catalyst companies and introduced into the market. Using co-impregnation in aqueous solution containing Co, Mo, orthosphosphoric acid and carboxylic acid and HY–Al_2O_3, Cosmo Oil Co. Ltd. developed C-606A with 3 times higher HDS activity compared to the conventional CoMoP/Al_2O_3 [18]. Akzo Nobel came up with the STARS catalyst series [17], which almost doubled the HDS activity. In recent time, the company introduced to the market a new catalyst, the NEBULA, which is considered a breakthrough in hydrotreating catalysts [19]. The new catalyst is made of unsupported bulk sulfides of group VIII and group VI metals which is almost 4 times as active as conventional gas oil hydrotreating catalysts. ART has introduced the sulfur minimization by ART (SMART) catalyst system, with a remarkably higher activity than predecessor hydrotreating catalysts [20].

A number of catalysts such as TK-573, TK-574, TK-911 and TK-915, not only significantly improved desulfurization activity, but also tackled density and aromatics reduction, have been developed by Topsøe. Recently, Topsøe has developed a new catalyst preparation technology, giving highly active hydroprocessing catalysts. This new proprietary BRIM technology not only optimizes the brim site hydrogenation functionally, but also increases the type II activity sites for direct desulfurization [21]. The first two commercial catalysts based on the brim technology were Topsøe's TK-558 BRIM (CoMo) and TK-559 BRIM (NiMo) for FCC pretreatment service. This was followed by a new series of high performance TK-576 BRIM (CoMo), TK-575 BRIM (NiMo) and TK-605 BRIM catalysts for ultra low sulfur gasoline production and for hydrocracker feed pretreatment [17]. Research on developing improved catalyst for desulfurization is an active research area and is expected to continue to play a key role in achieving the clean fuel agenda.

2.2 Preparation Methods

The performance of a catalyst is strongly influenced by preparation procedures [22]. Typical HDS catalyst preparation involves the use of incipient-wetness or pore-volume impregnation of an aqueous Mo-solution. As mentioned, high Mo loading and dispersion cannot be obtained by such a procedure because the formation of large particles occurs readily under the activation conditions [5]. Attempts to increase the loading of the active phase include the reduction of ammonium tetrathiomolybdate $(NH_4)_2MoS_4$ by hydrazine in aqueous solution in the presence of alumina particles which is reported to lead to the formation of highly dispersed MoS_2 supported on Al_2O_3 [23]. Another method for preparing an active HDS catalyst is a sonochemical synthesis, which was demonstrated to yield substantially high loading and dispersion of MoS_2 [24]. Moon et al. reported that sonochemically prepared MoS_2/Al_2O_3, at a Mo loading of 25 wt.%, showed a five-fold higher activity than that of a corresponding catalyst prepared by a conventional impregnation method in the HDS of model DBT compounds [24]. Another method for improving catalyst activity is to introduce a promoter, e.g., Co, to MoS_2 catalysts by chemical vapor deposition (CVD) such that the promoter interacts intimately with the MoS_2 surface. For example, a catalyst prepared by thermodecomposition of $Co(CO)_3(NO)$ on MoS_2/Al_2O_3 showed twice as high an activity as the catalyst promoted by impregnation in the HDS of thiophene [25]. The enhanced activity can be attributed to the exclusive decoration of Co on MoS_2 edge sites, which eventually leads to an increase in the amount of catalytically active CoMoS phase. Similar results were obtained by Okamoto et al. [26] with model CoMoS catalysts supported on various supports, which were prepared using the CVD method. More recently, Moon et al. [24], combined sonochemical synthesis and CVD to prepare new highly dispersed and promoted catalysts.

The amount and dispersion of the deposited molybdate will, of course, be controlled by the nature of the molybdenum solution used. The speciation of molybdenum in aqueous solution is dependent on the concentration of the Mo ions in solution and the pH of the solution, and is determined by the following equilibrium scheme [27]:

$$7MoO_4^{2-} + 8H^+ \leftrightarrow Mo_7O_{24}^{6-} + 4H_2O \qquad (a)$$

$$7MoO_4^{2-} + 9H^+ \leftrightarrow HMo_7O_{24}^{5-} + 4H_2O \qquad (b)$$

$$7MoO_4^{2-} + 10H^+ \leftrightarrow H_2Mo_7O_{24}^{4-} + 4H_2O \qquad (c)$$

At high pH values, the oxo-molybdenum species MoO_4^{2-} and $Mo7O_{24}^{6-}$ are the main Mo-species present in the solution, with greater amounts of the former [27]. Hydrothermal reaction in this case will not lead to the formation of extensive amounts of large, agglomerated particles [28]. The particles deposited onto the surface of the support in this case will be the result of an ion exchange process with the polyelectrolyte [8]. However, at lower pH values the molybdenum hydroxo-oxo complexes are present in appreciable amounts, and under hydrothermal conditions extensive oxolation would occur. This in turn leads to the condensation of large and agglomerated molybdate particles [28]. Therefore, by controlling the Mo concentration and the pH of the solution, the amount and dispersion of the deposited molybdate on a given polyelectrolyte multilayer can be fined tuned [8].

2.3 Supported Catalysts

For several decades, CoMo and NiMo/alumina have been used in industrial refining plants as HDS catalysts. Since the proposal of Topsøe and co-workers [29], there has been a growing interest in the so-called CoMoS or NiMoS phases, in which Co(Ni) decorates the edge sites of highly dispersed MoS_2 particles. These phases may be catalytically active sites in Co(Ni)–Mo sulfide catalysts and many catalytic and spectroscopic aspects of Co(Ni)–Mo sulfide catalysts have been interpreted in terms of these phases. Candia et al. [30] differentiated between two CoMoS phases, Type I and Type II, depending on their intrinsic HDS activity. CoMoS Type II, which was formed by high-temperature sulfidation at ~600-1000 °C, was about twice as active as Type I formed by sulfidation at ~400 °C. Transmission electron microscopy (TEM) and X-ray photoelectron spectroscopy (XPS) analyses showed that changes in the stacking number of MoS_2 slabs lead to the different types of CoMoS phases [31]. Accordingly, the formation of highly dispersed CoMoS Type II may result in highly active Co–Mo sulfide catalysts. Hence, the control of the morphology, size and stacking number, of supported MoS_2 particles is of paramount importance for the design of highly active HDS catalysts.

2.4 Catalyst Loading

Much less is known of this route, namely, creating the nanoparticles directly at the surface of a support. This method involves the growth of the nanoparticles from a precursor solution in the presence of a support that is covered by polyelectrolyte multilayers or brushes. In this way the polyelectrolyte-covered surface of the support becomes a “nano-reactor” in which particle growth is done. This way of generating nanoparticles is comparable to the use of micelles or dendrimers [32] as “nanoreactor”. The use of polyelectrolyte brushes or multilayers as nanoreactors has a number of clear advantages. It has been reported that a high concentration of ions are confined or immobilized in the brush layer. This confinement was predicted some time ago by Pincus to “close” the nanoreactor and prevent the formation of solid particles in the solution phase [10]. Moreover, our experience with such method in the growth of zeolitic particles on macroporous carbon has revealed that the initial solution confinement in the polyelectrolyte layers leads to the formation of nanoparticles that are anchored to the surface of the support. This is realized through the formation of a “transition layer” that acts as roots anchoring the nano-particles to the walls of the support. This, in turn, has stabilized the nano-particles against agglomeration and loss of the exposed active surface area during calcinations and/or exposure to the reaction condition.

2.5 Supported Mo Catalyst and HDS Reaction of Model Compounds

The removal of sulfur from gasoline and diesel oil is becoming more and more necessary due to the implementation of more stringent specifications in many countries. By comparing gas chromatographic analysis of hydrotreated gas oils to that of the corresponding straight-run gas oils shows clearly that alkyldibenzothiophenes and particularly 4,6-dimethyldibenzothiophene (4,6-DMDBT) are the sulfur impurities that are the most difficult to decompose [5,33]. Actually, on typical CoMo/alumina and NiMo/alumina hydrotreating catalysts, 4,6-DMDBT was found to be much less reactive than dibenzothiophene (DBT) [34-36]. It has been suspected for a long time that the low reactivity of 4,6-DMDBT was due to steric effects on adsorption.

The product distribution obtained in DBT HDS over typical CoMo and NiMo/alumina catalysts shows that the reaction gives essentially two families of products: biphenyl-type compounds and tetrahydrodibenzothiophene-type compounds [37,35]. The latter in turn lead to cyclohexylbenzene-type products. Moreover, it has been shown that, under HDS conditions (i.e., in the presence of an organic sulfur compound), biphenyl-type compounds do not hydrogenate readily into cyclohexylbenzene [38,35]. Despite the fact that this point is still questioned especially with NiMo catalysts [5], it was concluded that the HDS of DBT-type compounds occurred through two parallel reactions as indicated in Scheme 1: (i) direct desulfurization (DDS) which yields biphenyl-type compounds, and (ii) desulfurization through hydrogenation (HYD) which gives first tetrahydrodibenzothiophene and then cyclohexylbenzene-type compounds.

For the DDS pathway, one way to obtain a C–S bond cleavage ending with two phenyl rings in the product is to hydrogenate one of the double bonds in the vicinity of the sulfur atom to obtain a dihydrogenated product and then to open the C-S bond by an elimination process, Scheme 1 [34]. It is noted that this particular double bond is not necessarily the easiest to be reduced. The second C–S bond cleavage leading to the biphenyl compound possibly occurs through the same mechanism. However another possibility of obtaining a C–S bond cleavage ending with aromatic rings is the insertion of a metal atom in the C–S bond [39]. This step has been reported to be sensitive to steric hindrance.

For the HYD pathway, which involves the hydrogenation of one aromatic ring, it is reasonable to consider a step-by-step process beginning also with the hydrogenation of the substrate into a dihydrogenated intermediate. Therefore, as proposed earlier [34], it has been assumed that the two pathways have dihydrodibenzothiophene compounds as intermediates (Scheme 1). It is also noted that, whatever the reactant, the second C–S bond cleavage in the HYD pathway does not require the second aromatic ring to be fully hydrogenated and may occur through a DDS-type process leading to the production of cyclohexylbenzene instead of dicyclohexyl-type compounds. This means that the second C–S bond cleavage is not affected much by the presence of a methyl group in the vicinity of the sulfur atom in the second aromatic ring [40].

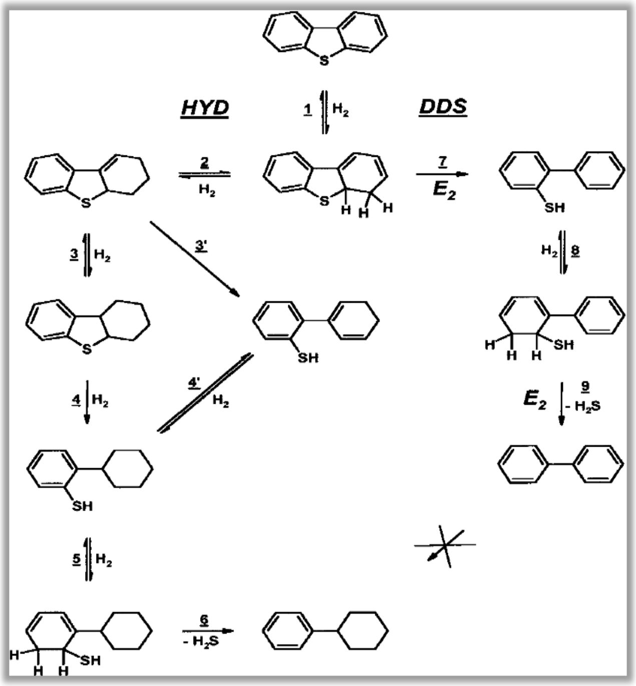

Figure 1:Reaction scheme for the hydrodesulfurization of DBT [40].

In the literature, many of the results reported on alkylated thiophene HDS have been obtained with promoted hydrotreating catalysts, namely sulfided CoMo and NiMo/alumina catalysts. Considering the important promoter effect often measured for hydrotreating reactions, it appears of importance to know how the observations summarized above can be influenced by the presence of promoted and highly dispersed small MoS_2 particles.

2.6 Statement of Problems

a) It is of great importance to control the Mo concentration and the pH of the solution. By controlling these parameters, the amount and dispersion of the deposited molybdate on a given polyelectrolyte multilayers can be fine-tuned [8].

b) The control of the morphology, size and stacking number of supported MoS_2 particles is of paramount importance for the design of highly active HDS catalysts.

c) The use of polyelectrolyte brushes or multilayers as nano-reactors has a number of clear advantages. It has been reported that a high concentration of ions are confined or immobilized in the brush layer. This confinement was predicted some time ago by Pincus to “close” the nano-reactor and prevent the formation of solid particles in the solution phase [10]. Moreover, our experience with such method in the growth of zeolitic particles on macroporous carbon has revealed that the initial solution confinement in the polyelectrolyte layers leads to the formation of nanoparticles that are anchored to the surface of the support. This is realized through the formation of a "transition layer" that acts as roots anchoring the nano-particles to the walls of the support. This, in turn, has stabilized the nano-particles against agglomeration and loss of the exposed active surface area during calcinations and/or exposure to the reaction condition.

CHAPTER 3

EXPERIMENTAL METHODS

3.1 Proposed Catalyst Preparation

The overall catalyst preparation procedure and the final product $CoMoS_2/\gamma{-}Al_2O_3$ is shown in the figure below:

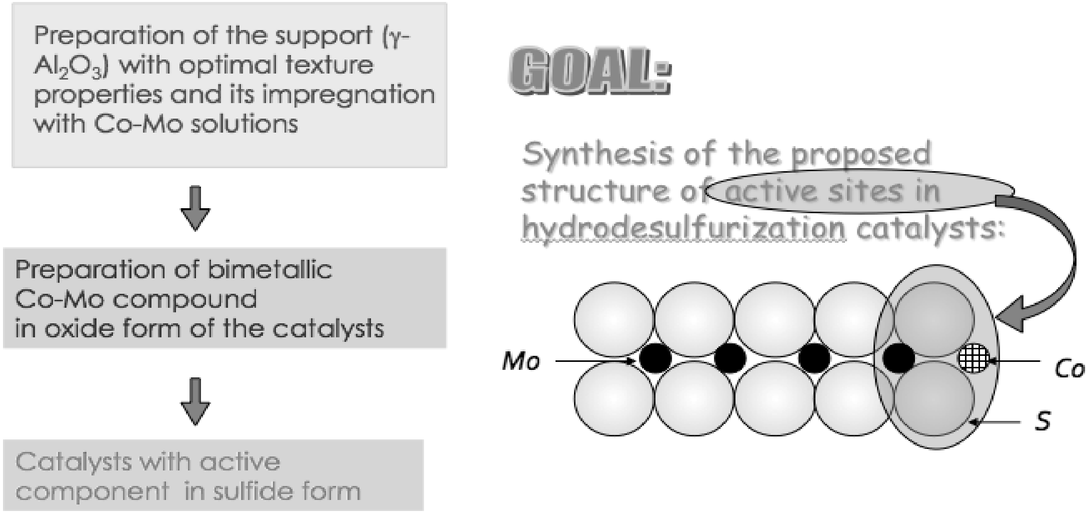

Figure 2: The schematic representation shows the overall methodology of the proposed catalyst.

The following shoes all the steps of forming the proposed catalyst in detail:

3.1.1 Synthesis of the Support and polyelectrolyte-coated γ-Al_2O_3

γ-Al_2O_3 was synthesized from boehmite using pipitization method. The resulting gel is cooled and freeze-dried and subsequently calcined at 550 °C to afford γ-Al_2O_3. The γ-Al_2O_3 is coated alternately with aqueous solutions of cationic and anionic polymer to afford polyelectrolyte-coated support. The synthesis initially involved the formation of polyelectrolyte multilayer on the surface of the γ-Al_2O_3 where the first polyelectrolyte layer was chosen to be made of a negatively charged polymer poly(sodium-4-styrenesulfonate) (PSS, Aldrich, Mw = 70,000)) deposited from a solution with a concentration of 4 mg ml^{-1} and a pH value of about 8.4. This step was carried out by soaking 60 g of γ-Al_2O_3 in 30 ml aqueous solution of PSS for 2 h. Subsequently, six more polyelectrolyte layers of alternating charges were placed, starting with a negatively charged deposited from an aqueous solution and ending with a positively charged polyelectrolyte outer layer poly(diallydimethylammonium chloride) (PDDA, Aldrich, Mw=100,000–200,000) deposited from a 4 mg ml^{-1} aqueous solution of. The γ-Al_2O_3 uptake of both polyelectrolytes was verified by TGA.

3.1.2 Loading of Mo:

The polyelectrolyte-coated γ-Al_2O_3 was soaked in aqueous solutions of ammonium heptamolybdate tetrahydrate, $(NH_4)_6Mo_7O_{24}.4H_2O$ (Fischer Scientific), with Mo-concentrations of ranging from 0.1M to 0.5M at pH values of 4,6, & 8. The materials were dried in air over night and then filtered to get the final product which is Mo dispersed on polyelectrolyte-coated γ-Al_2O_3. The amount of Mo-loaded was determined by ICP by taking 5 ml of the solution after filtration and fill the flask to 100 ml by the addition of deionized water. Then, the material was calcined in air at 500 °C for 4 h. Subsequently; the chemical nature of the loaded Mo-species was investigated by Raman spectroscopy.

3.1.3 Promoter Loading:

All γ-Al_2O_3 supported samples containing MoO_3 (denoted Mo/Al_2O_3) at fixed pH value equals to 5.5 were impregnated by aqueous solution of Co containing the required amounts of $Co(NO_3)_2.6H_2O$ with these concentrations 0.005, 0.01, 0.025, 0.05, 0.1, 0.15 and 0.2. The amount of Co-loaded was determined by ICP by taking 5 ml of the solution after filtration and fill the flask to 100 ml by the addition of deionized water. All catalysts were subsequently dried in airflow for 24 h at room temperature and then calcined in air at 500 °C during 4 h.

3.2 Standard Catalyst Preparation:

A standard Co/Mo/γ-Al_2O_3 hydrodesulfurization catalyst was synthesized by impregnation for comparison purpose as follows: about 10g of calcined pure γ-Al_2O_3

was impregnated with an 25 ml of aqueous solution of the 1.836 g molybdenum precursor, $(NH_4)_6Mo_7O_{24}$, at pH = 4. The wet solid was then dried at 100 °C for 16 h and calcined in air under static conditions at 500°C for 4 h using a ramp step of 2°C per min. Next, the final material was impregnated by 25 ml solution of 0.438 g of cobalt precursor, $Co(NO_3)_2.6H_2O$, dissolved in deionized water. The wet product was dried at 200 °C for 24 h and calcined in air at 500°C for 4 h using a ramp step of 2°C per min.

3.3 Sulfidation of Synthesized Catalysts:

The sulfidation protocol differs from large-scale industrial settings to a laboratory scale. In the laboratory, a mixture of H_2/H_2S is usually employed for the sulfidation of oxide catalysts under a control temperature program. The process can be ex situ or in situ. So, before the catalytic activity tests, the catalysts were sulfided ex situ in a tubular furnace at 400°C for 2 hours in a stream of 10% H_2S in a balanced H_2. The presulfiding step is necessary to convert the catalyst from oxide form to sulfide form, which is the active site under the conventional reaction system. The sulfided catalyst was transferred quickly into the reactor tube. Catalysts were then tested in the HDS of 2methylethiophene (Sigma–Aldrich, 98%) using a continuous-flow high-pressure fixed-bed reactor.

3.4 Catalyst Characterization:

3.4.1 Inductively Coupled Plasma (ICP)

A method for the determination of Mo and Co using inductively coupled plasma (ICP) of the synthesized catalysts was used. The concentrations of both Mo and Co were efficiently determined after catalyst acid digestion with 10% (v/v) hydrochloric acid and heating (160 degrees C for 24 h) and sonication (during 2 min). The Mo and Co detection limits are 0.002% and 0.08%, respectively, using 0.20 g of catalyst sample in 50 ml.

3.4.2 Acid – Base Properties by NH_3-TPD:

Temperature – Programmed Desorption (TPD) of NH_3 measured the surface acidity of solid catalysts. It was carried out in a Quantachrome Autosorb-1c. In the TPD experiments, the sample, after drying at 300 °C, was saturated with 10% NH_3/He (15 ml/min) at 50 °C for 1h, and then was purged with pure He for 1h. For desorption, it was heated (10 °C/min) to 700 °C in flowing He (25 ml/min), and monitored with mass spectrometer.

3.4.3 Raman Spectroscopy:

Raman Spectroscopy has probably been the greatest contributor to the rapid progress in the area of supported metal oxide catalysts characterization, because of its ability to discriminate between metal oxide structures and its in situ capabilities. The support alumina showed no specific peaks in Raman spectroscopy. A number of studies on the assignment of Raman band positions have been reported for supported molybdenum catalysts.

3.4.4 X-ray Photoelectron Spectroscopy (XPS):

XPS analyses were performed on samples of the catalysts in the sulfide states with a Kratos Axis Ultra spectrometer (Kratos Analytical, Manchester, UK) equipped with a monochromatized Al X-ray source (powered at 10 mA and 15 kV). The sample powders were pressed into small stainless steel troughs mounted on a multi-specimen holder. The pressure in the analysis chamber was around 10^{-6} Pa. The angle between the normal to the sample surface and the lens axis was 0°. The hybrid lens magnification mode was used with the slot aperture resulting in an analyzed area of 700 µm × 300 µm. The pass energy was set at 40 eV. In these conditions, the energy resolution gives a full width at half maximum (FWHM) of the Ag $3d_{5/2}$ peak of about 1.0 eV. Charge stabilization was achieved by using the Kratos Axis device.

3.4.5 Brunauer, Emmett and Teller (BET) and Barrett-Joyner-Halenda (BJH) methods:

The specific surface area, pore size, and pore size distribution of the samples were analyzed based on he nitrogen adsorption isotherm measured at -196 ^{o}C using a Quantachrome-Autosrob-1c. Samples were degassed at 120 ^{o}C for 3 h prior to analysis. Specific surface area of the developed catalysts was calculated using the BET method. The pore distribution and mean pore size of the desorption branches of nitrogen adsorption isotherms were calculated using BJH method.

3.4.6 Transmission Electron Microscopy (TEM):

Transmission electron microscopy (TEM) is an analytical technique used to characterize the morphology, size and crystal structure of materials such as catalysts. Electrons have wave like characteristics, with a wavelength substantially less than visible light. Since electrons are smaller than atoms, TEM is capable of resolving atomic level detail. The microstructural characteristics and selected area electron diffraction (SAED) of the samples were identified using JEOL-2000 EX II high-resolution transmission electron microscope operated at 200 kV.

The specimen for the TEM study was prepared by suspending the powder sample in methanol. The powder sample was ultra-sonicated in a methanol medium and one drop of the suspension was loaded on the carbon-coated grids. These samples loaded grids were dried under a lamp for over 1 hour under ambient conditions and loaded into the specimen carousel. Phase identification has been attempted based on analysis of the electron diffraction patterns.

3.4.7 Thermal Gravimetric Analysis (TGA):

Electrolyte uptake by γ-Al_2O_3 was examined on a thermo-gravimetric analyzer (TGA), an instrument capable of simultaneous TGA/DSC analysis (TA Instruments). In a typical thermo-gravimetric analysis, approximately 20 mg of sample was placed in a crucible and purged with nitrogen at 30 ^{o}C for 30 min at the flow rate of 100 mL/min, and then the heating was ramped at 10 ^{o}C/min to 400 ^{o}C under the flow of air at 100 mL/min.

3.4.8 Gas – Chromatography (GC):

Gas chromatography (GC) is a commonly used analytical technique in many research and industrial laboratories. A broad variety of samples can be analyzed as long as the compounds are sufficiently thermal stable and volatile enough. The products coming out from the reactor were analyzed by GC. The GC used has two detectors namely, flame ionization detector (FID) and thermal conductivity detector (TCD). These detectors are sensitive towards organic molecules, the TCD 10-^{5}-10-^{6}g/s (linear range: 10^{3}-10^{4}) and FID 10^{-12} g/s (linear range: 10^{6} –10^{7}).

3.4.9 Instrument Set-up for HDS and HYD reactions and components of synthetic FFC gasoline:

The 2-methylthiophene (for HDS) and 2,3MethylBut-2-ene (for HYD) tests under lab conditions were carried out in a fixed-bed tubular stainless-steal reactor (34 cm long, 4 mm i.d.) with an axial thermo well containing a thermocouple centered in the catalyst bed. The required amount of catalyst precursor to yield 0.20 g of oxidic precursor (<250 μm) was loaded between quartz wool plugs. The activation or sulfurisation process was made using a hydrogen sulfide flow (ultra high purity) of 20 cm^3 min^{-1} controlled by a mass flow meter. The composition of the liquid hydrocarbons is shown in the following table:

Table 1 The synthetic FCC gasoline components and their quantities.

Components of model FCC gasoline	
2-methylthiophene	3 wt%
2,3-dimethylbut-2-ene	20 wt%
o-Xylene	30 wt%
n-Heptane	47 wt%

Reaction conditions were similar to those of typical HDS processes: T = 498 K, P = 20 bar, and H_2/liquid hydrocarbon feed ratio of 200 L/L as illustrated in Table 2. The absence of any diffusion limitations was previously verified. Liquid products were analyzed using a HP 6890 GC equipped with an FID, an HP-1 capillary column (100 m × 0.25 mm × 0.5 μm) and a split injector. Catalytic tests were conducted until reaching the steady state. Reaction products detected were: 2-methylthiophene and 2,3MethylBut-2-ene. The experimental configuration is shown in figure 3.

Table 2 Overall reaction conditions:

Reaction parameters	
Catalyst weight (g)	2
Feed	Synthetic FCC gasoline
H_2 Pressure (bar)	20
H_2/hydrocarbon (L/L)	200
Liquid hourly space (h^{-1})	3
Feed flow (ml/min)	0.134
H_2 flow (ml/min)	26.8
Reaction temperature (°C)	225
Duration (h)	9

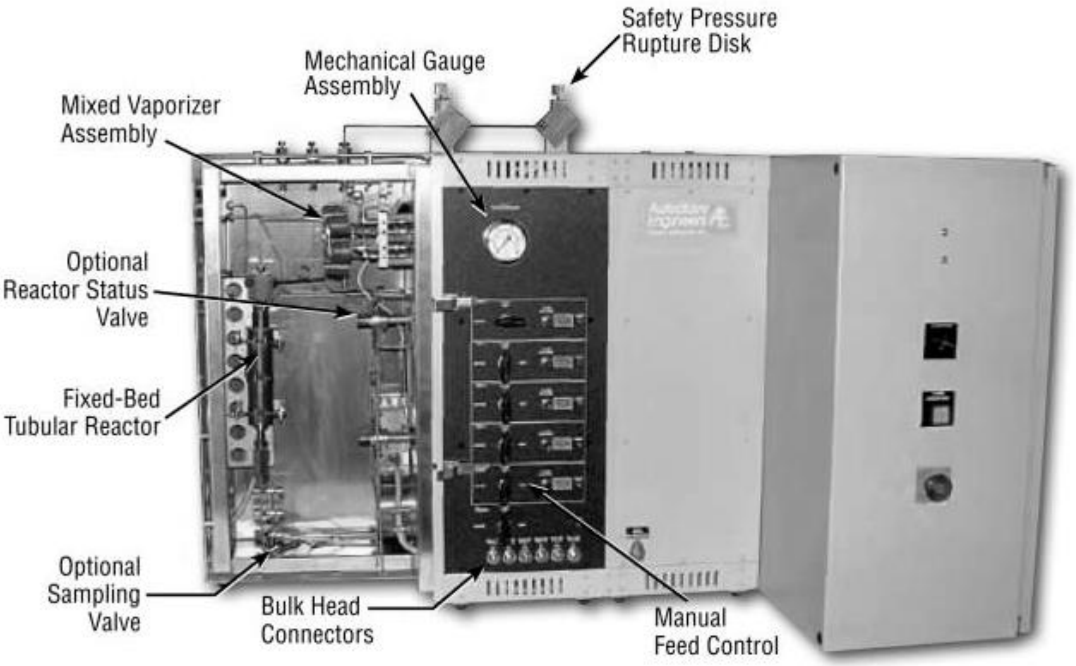

Figure 3 Picture illustrates the main parts of the device used for HDS and HYD tests.

CHAPTER 4

RESULTS AND DISCUSSIONS

4.1 γ-Al_2O_3 Support Coating

A support material (γ-Al_2O_3) was prepared with optimal texture properties and coated alternately with two different kind of polyelectrolyte namely, poly (sodium(IV)-styrenesulfonate) (-ev) and poly (diallyldimethylammoniumchloride) (+ev). The coating was done till five different layers have been achieved as indicated by the TGA results, shown in Figure 3.

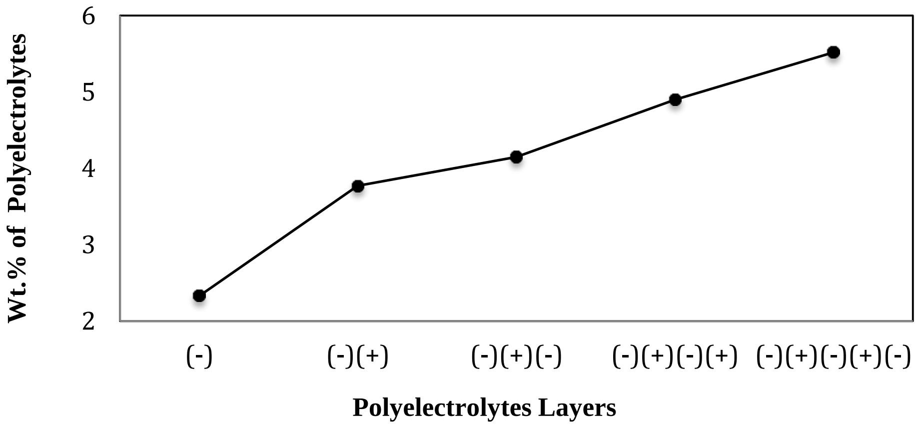

Figure 4: TGA analysis of different layers of two kind of Polyelectrolyte on Al_2O_3.

Subsequently, the coated alumina was impregnated with molybdenum solutions of same concentration (0.5M) at different PH values: 4, 6 and 8. The speciation of molybdenum in aqueous solution is dependent on the pH and concentration of the solution, and is determined by the following equilibrium equations [27]:

At pH = 8 $7MoO_4^{2-} + 8H+ \leftrightarrow Mo_7O_{24}^{6-} + 4H_2O$ (a)

At pH = 6 $7MoO_4^{2-} + 9H+ \leftrightarrow HMo_7O_{24}^{5-} + 4H_2O$ (b)

At pH = 4 &6 $7MoO_4^{2-} + 10H+ \leftrightarrow H_2Mo_7O_{24}^{4-} + 4H_2O$ (c)

This has been confirmed by analyzing the samples by using Raman spectroscopy as shown in Figure 4. At pH= 4 and 6, the material shows a peak at 980 cm^{-1}, which can be attributed to high metal content and to the large polymeric octahedral $H_2Mo_7O_{24}^{4-}$ and $HMo_7O_{24}^{5-}$ clusters, respectively. In the case of catalysts prepared at pH= 8, this peak was found to be less intense suggesting the formation of less octahedral $Mo_7O_{24}^{6-}$ clusters and more tetrahedral MoO_4^{2-} species. A strong peak at 920 cm^{-1} was observed in catalyst prepared at pH= 8, and can be assigned to the MoO_4^{2-} in tetrahedral coordination.

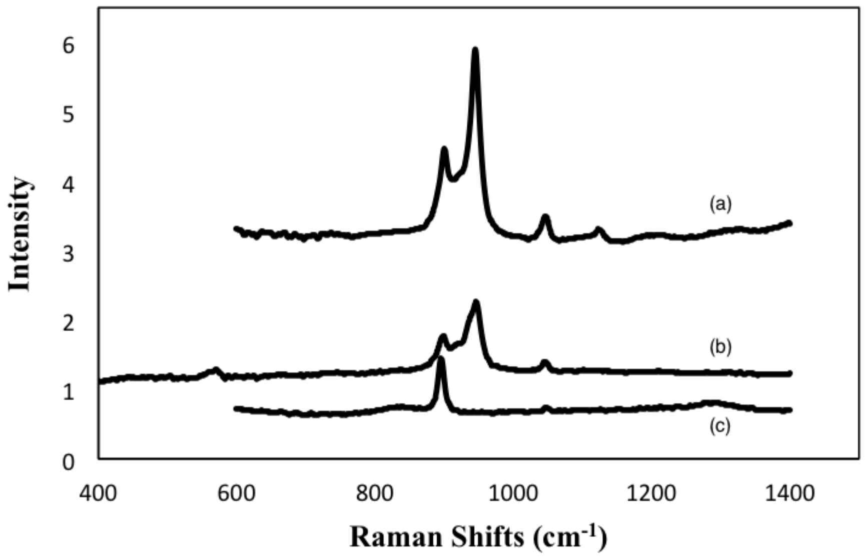

Figure 5: Raman spectra for Mo species at (a) pH = 4, (b) pH = 6 and (c) pH = 8

Additionally, the coated alumina has been further loaded with Mo solutions at different concentrations ranging from 0.1M to 0.5M at same pH= 6. The following Raman spectra were obtained which show the effect of varying the concentration:

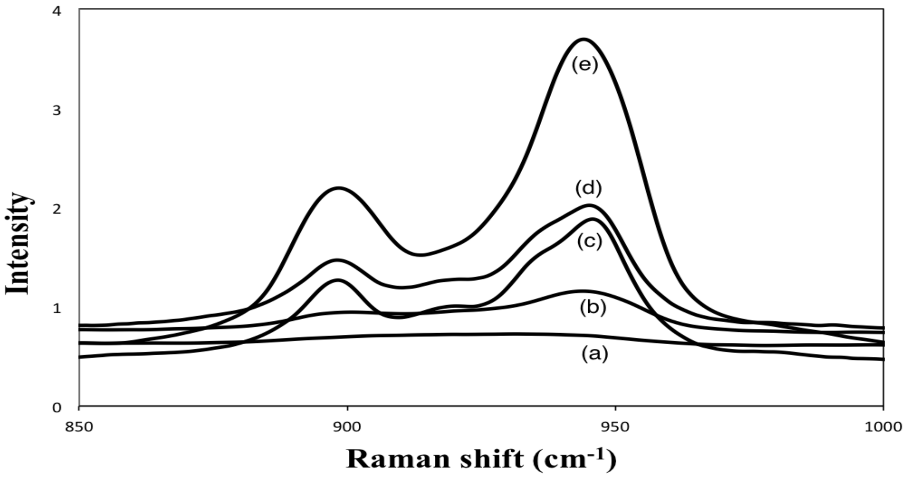

Figure 6: Raman spectra for Mo species at pH = 6 for concentrations of (a) 0.1 M, (b) 0.2 M, (c) 0.3 M, (d) 0.4 M and (e) 0.5 M.

From figure 5, it can be concluded that the speciation of molybdenum in aqueous solution was not affected by the concentration of the solution. This result is indicative of an ion-exchange process where no excess Mo-species was found to form. Moreover, the same-coated alumina [(-ve) and (+ve)] was soaked with different concentrations varying from 0.1 to 0.5 and at different pH values: 4, 6 and 8. The uptake of negative and positive coated Al_2O_3 in these different Mo solutions was determined by using ICP-AES. The analyses of each were illustrated below in table 3 and figures 6-8:

Table 3: ICP analysis of (–ve) and (+ve) coated alumina in (0.1-0.5) M Mo solutions at pH= 4, 6 and 8.

Mo Concentration (M)	Negative- %Mo	Positive- %Mo	Negative- %Mo	Positive- %Mo	Negative- %Mo	Positive- %Mo
	pH= 4		pH= 6		pH= 8	
0.1	6.825	7.193	3.684	2.746	1.744	2.320
0.2	12.204	12.396	7.600	8.025	2.629	2.629
0.3	13.941	13.588	13.793	14.419	4.762	5.504
0.4	14.292	15.541	16.422	16.211	5.771	5.771
0.5	14.730	15.505	16.245	16.160	6.125	6.125

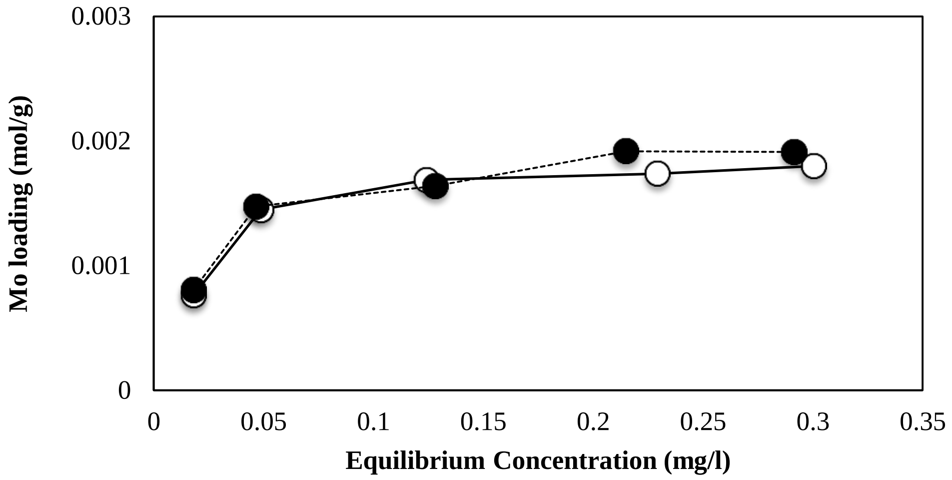

Figure 7: Uptake of negative (○) and positive (●) coated alumina in Mo solutions at pH = 4.

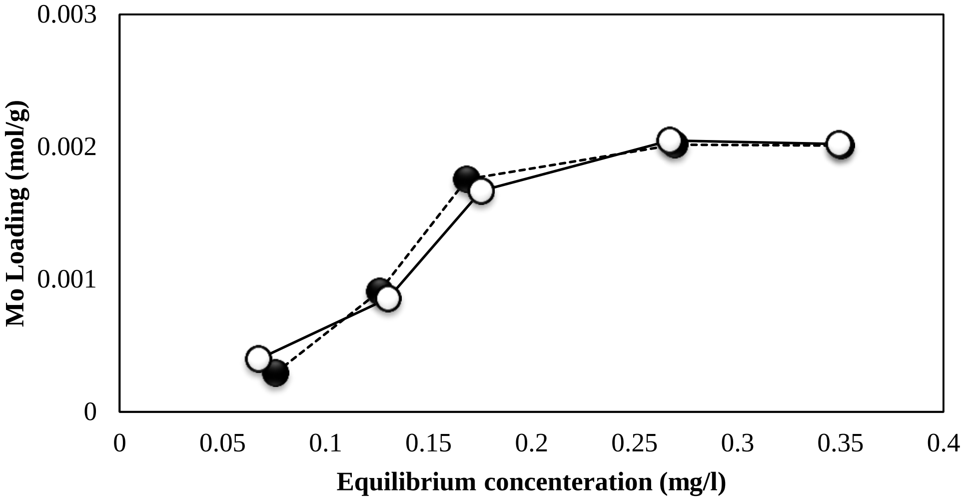

Figure 8: Uptake of negative (○) and positive (●) coated alumina in Mo solutions at pH 6.

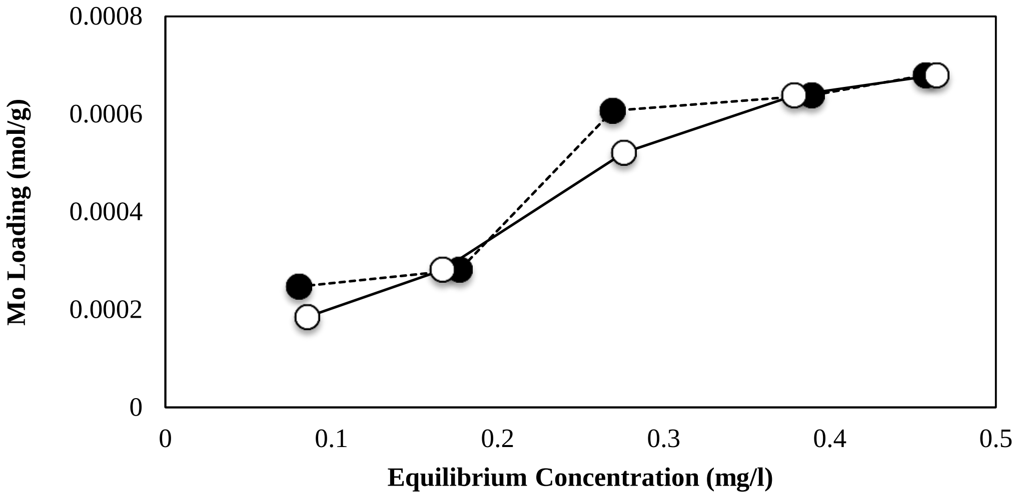

Figure 9: Uptake of negative (○) and positive (●) coated alumina in Mo solutions at pH 8.

It can be interpreted from the analysis that at pH 6, the high loading of Mo species has been achieved. Also, at pH= 4 the loading of Mo particles was very comparable to that of Mo concentration at pH= 6. In contrast, at pH= 8, Mo loading was very small compared with that of at pH= 6 and 4. The reason behind that decrease is that at pH= 8 the Mo species only exchange with Cl^- ions at positive polyelectrolyte. Hence, there were only two layers of positive polyelectrolyte, which were not enough to be loaded with Molybdenum. Therefore, increasing positive polyelectrolyte used for pH 8 loading will favor obtaining high loading of Mo. All in all, Mo species found onto polyelectrolyte coated γ–Al_2O_3 are as follows:

- At pH = 4, Mo species mainly $H_2Mo_7O_{24}^{4-}$
- At pH = 6, Mo species mainly $H_2Mo_7O_{24}^{5-}$ and $H_2Mo_7O_{24}^{4-}$

This drives us to the conclusion that both Mo species can easily displace hydrated Na ions on the polyelectrolyte (PSS).

- At pH = 8, Mo species mainly MoO_4^{2-}

And this tells us that the exchange of the nucleophilic Cl^- ions on the polyelectrolyte (PDDA) took place at this pH because of the negative Mo species. In addition, figure 9 shows the Mo loading at 5 layers electrolytes – coated γ–Al_2O_3 at different pH values.

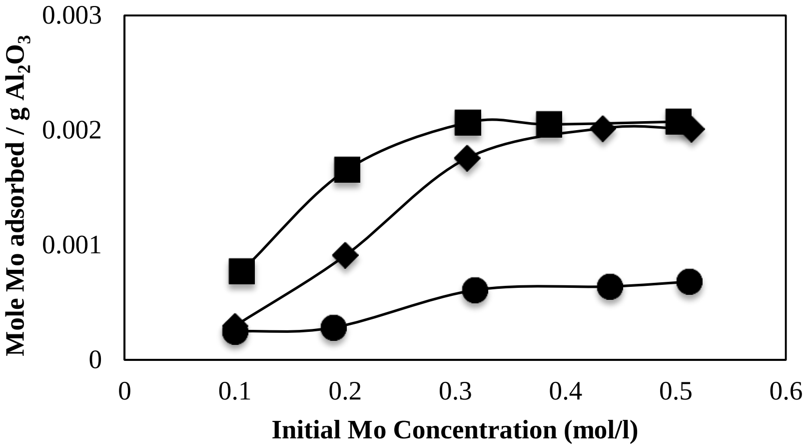

Figure 10: Mo content on (γ-Al_2O_3) at different concentration and pH value of 4 (■), 6 (◆) and 8 (●).

Lastly, the negatively coated alumina, that was loaded with Mo solution at pH 4 was soaked with aqueous solution of different concentration of Cobalt at pH= 5.5. And the uptake was determined by using ICP-AES technique. Table 4 and figure 10 below show the percentage of loading of both Mo and Co.

Table 4: The uptake of (–ve) coated alumina loaded with Mo at pH 4 and Co solutions at pH= 5.5.

Co concentration (M)	Co %	Mo %
0.005	0.249	10.4
0.01	0.274	10.3
0.025	0.375	9.8
0.05	0.744	9
0.1	1.02	8
0.15	1.38	6.8
0.2	1.77	5.8

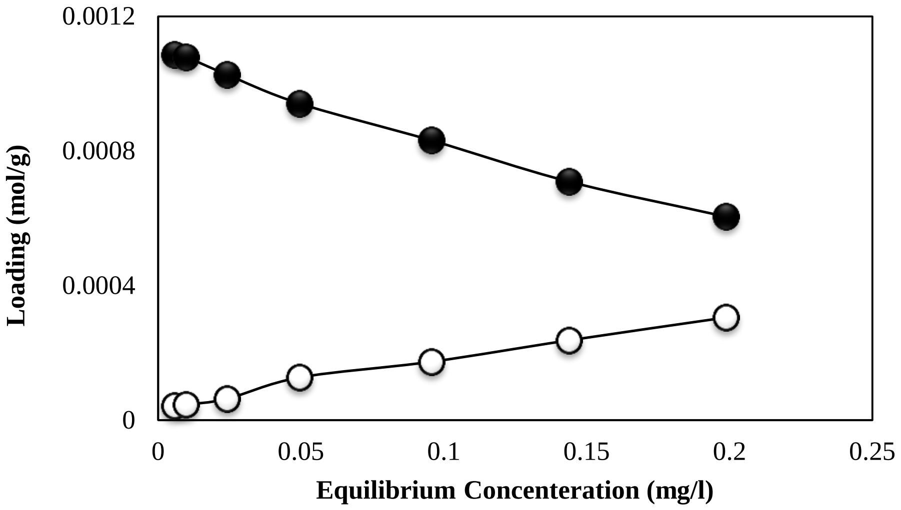

Figure 11: Uptake of (–ve) coated alumina in 0.4 M Mo (●) and different conc. of Co (○) at pH 5.5.

It is obvious that as the concentration of Co increases, the Mo concentration decreases. Co particles displaced some of the Mo species in all samples and the more Co particles up taken by the samples, the lesser Mo species will be. Consequently, a significant drop in Mo concentration would lead to less active catalyst. In order to tackle this problem, an increase of the positive polyelectrolyte would increase Mo uptake at pH= 8 while the negative polyelectrolyte would increase uptake the positively charged cobalt ion at pH 5.5. This will create no interference between the two metals. Hence, this will be the optimum way to obtain high loading of both Mo and Co.

Therefore, 5-layered polyelectrolyte coated alumina that were impregnated with Mo solution of 0.5 M at pH= 8, 6 and 4, respectively, were soaked in aqueous solutions of different concentrations of cobalt at pH= 5.5. The Co uptake was determined by using ICP-AES technique. Figures 11-13 below show the variation in content of both Mo and Co on these alumina systems and Table 5 lists the obtained loading values.

Table 5: Mo and Co amount in all catalysts before sulfidation.

Sample	Initial amount		Co/Mo Mol ratio	Mole Fraction Co
	Wt% Co	Wt% Mo		
pH4-0.4M-Mo	0	23.679	0	0
pH4-0.01M-Co	0.311	14.778	0.034	0.033
pH4-0.025M-Co	0.464	15.455	0.049	0.047
pH4-0.05M-Co	0.676	15.827	0.07	0.065
pH4-0.1M-Co	0.97	14.545	0.109	0.098
pH4-0.2M-Co	1.071	11.349	0.154	0.133
pH8-1-0.5M-Mo	0	10.776	0	0
pH8-1-0.01M-Co	0.441	8.513	0.084	0.078
pH8-1-0.025M-Co	0.659	8.699	0.123	0.11
pH8-1-0.05M-Co	0.781	8.477	0.15	0.13
pH8-1-0.1M-Co	1.197	8.933	0.218	0.179
pH8-1-0.2M-Co	1.563	8.698	0.292	0.226
pH6-0.4M_Mo	0	15.2	0	0
pH6-0.005M-Co	0.249	10.425	0.039	0.037
pH6- 0.01M-Co	0.274	10.35	0.043	0.041
pH6-0.025M-Co	0.374	9.85	0.062	0.058
pH6-0.05M-Co	0.744	9.025	0.134	0.118
pH6-0.1M-Co	1.015	7.975	0.207	0.172
pH6-0.15M-Co	1.381	6.8	0.331	0.248
pH6-0.2M-Co	1.768	5.8	0.496	0.332

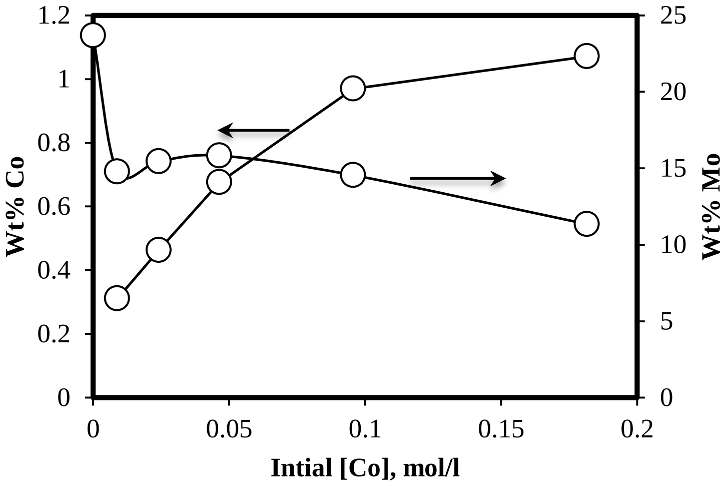

Figure 12: ICP analysis of Co loading compared with Mo loading at 0.4 M and pH= 4.

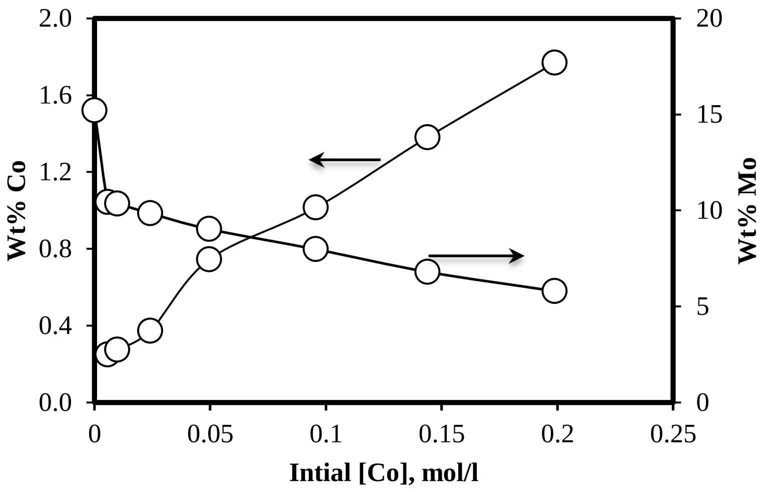

Figure 13: ICP analysis of Co loading compared with Mo loading at 0.4 M and pH= 6.

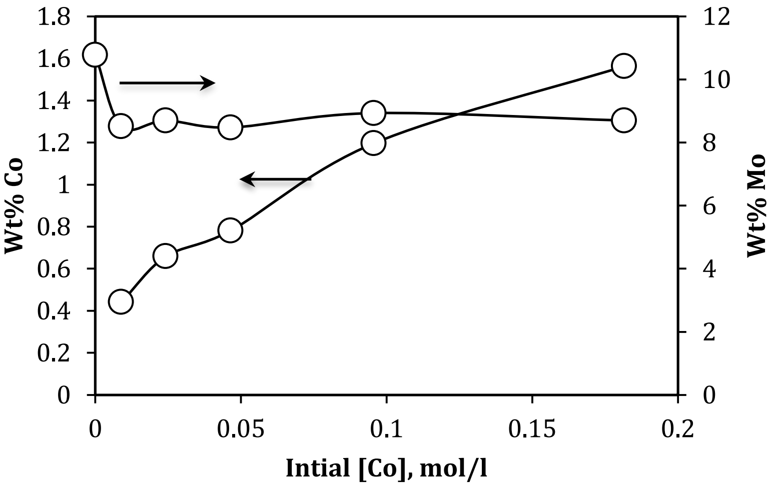

Figure 14: ICP analysis of Co loading compared with Mo loading at 0.4 M and pH= 8.

The following are the main observations that can be deduced from the above results:

- The Co species at pH = 5.5 is $CoOH^+$
- The $CoOH^+$ species is found to displace Mo loaded onto polyelectrolyte coated γ–Al_2O_3 at pH 6 and 4.
- $CoOH^+$ did not affect Mo loaded onto polyelectrolyte coated γ–Al_2O_3 at pH 8.

Of the prepared samples, three equivalent catalysts, those with almost the same Co/Mo mol ratio at different pH, were chosen and a reference catalyst was prepared for comparison. These catalysts have Co/Mo mol ratio about 0.15, as shown in Table 5. Consequently, the chosen catalysts and the standard one were crushed to obtain meshed materials between 200 and 300 μm. Then, they were sulfided in 10% vol H_2S/H_2 at 400 °C for 2h with heating rate of 5 °C/min. The sulfided materials were subjected to HDS and HYD tests on the FCC gasoline model. Before conducting the HDS and HYD tests, the physiochemical properties of all catalysts were studied by using N_2 adsorption/desorption, NH_3-TPD, TEM and other various analytical techniques.

4.2 N_2 Absorption / Desorption:

Nitrogen adsorption/desorption isotherms formed are, as shown in Figure 14, according to the BDDT classification, of type IV with an H_2 type (IUPAC) hysteresis attributed to the present disordered mesopores [41].

The main textural parameters of the samples are reported in Table 6. It is noticed that the BET surface area decreases from ~271 for the plain γ-Al_2O_3 support, to ~189 m^2/g with the presence of the supported metal sulfide catalysts. The total pore volume of the materials was also found to decrease with the addition of the metal sulfides and the extent of decrease in pore volume was relatively higher for the standard CoMo/γ-Al_2O_3 catalysts. Mono-model pore size distribution was obtained for all the catalysts, as shown in Figure 15. An average pore diameter of ~4.3 nm was basically the same for all catalysts that used polyelectrolyte multilayer to load the metal, and this value is less than that of the plain γ-Al_2O_3 support and and higher than that found for the standard CoMo/γ-Al_2O_3 catalyst. These results indicate metal loading via the polyelectrolyte multilayer have produced relatively low mesopore blockage when compared to the conventional impregnation method used, which in turn point to improved metal dispersion on the support.

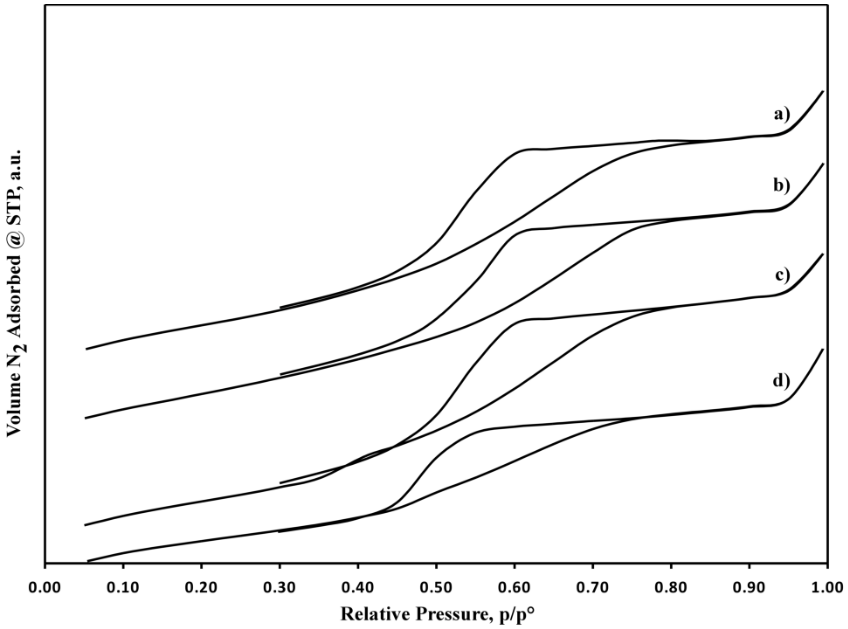

Figure 15: Nitrogen adsorption/desorption isotherms of sulfide a) Std. CoMo/ γ-Al_2O_3, b) pH4-0.4M_Mo_0.2M_Co, c) pH6-0.4M_Mo_0.05M_Co, and d) pH8-0.5M_Mo_0.05M_Co.

Table 6: Overall quantitative results of some physiochemical properties.

Sample	Mo	Co	SA	V_P	D_p	NH_3**
	(wt %)	(wt %)	(m^2/g)	(cm^3/g)	(nm)	(μmol g^{-1})
Plain γ-Al_2O_3*	NA	NA	271.0	0.36	4.95	NA
Std. CoMo/ γ-Al_2O_3	9.0	0.85	184.6	0.24	3.83	3010
pH4-0.4M_Mo_0.2M_Co	11.3	1.07	189.8	0.29	4.38	2251
pH6-0.4M_Mo_0.05M_Co	9.0	0.74	186.0	0.27	4.29	2201
pH8-0.5M_Mo_0.05M_Co	8.5	0.78	189.2	0.28	4.32	2032

* Unsulfided, γ-alumina support.

** Density of acid sites measured by Ammonia TPD.

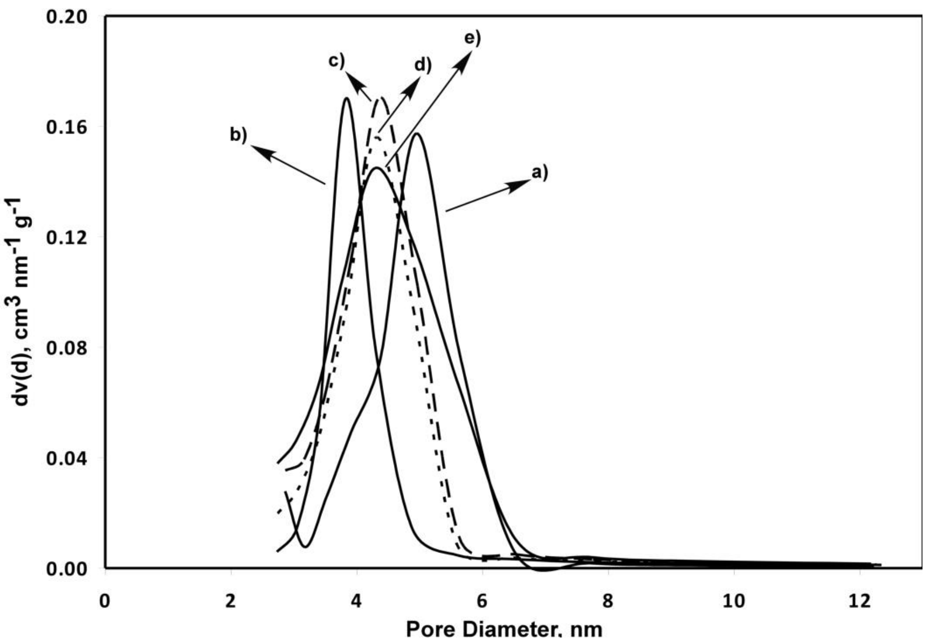

Figure 16: Pore Size distribution calculated by the BJH method using the desorption branch of the isotherm for a) γ-Al_2O_3, and the sulfide catalysts b) Std. CoMo/γ-Al_2O_3, c) pH4-0.4M_Mo_0.2M_Co, d) pH8-0.5M_Mo_0.05M_Co, and e) pH6-0.4M_Mo_0.05M_Co.

4.3 Ammonia Temperature Programmed Desorption (TPD):

NH_3-TPD profiles for the catalysts are depicted in Figure 16 and Table 6 lists the obtained quantitative results. It is noticed that the temperature at the maximum of the TPD peak and the density of acid sites are found to be higher for the standard CoMo/γ-Al_2O_3 catalyst, which is indicative of the formation of larger amounts and stronger NH_3-adsorbing acid sites. On the other hand, both the temperature at the maximum of the TPD peak and the density of the acid sites are found to decrease significantly for the sulfide catalysts prepared using the polyelectrolyte multilayer method. Hence, it seems that upon sulfidation of the catalysts prepared using the polyelectrolyte multilayer method, the remnants of the polyelectrolyte multilayer have neutralized a significant amount of the strong acid sites, in particular, and reduced the density of acid sites on catalysts, in general.

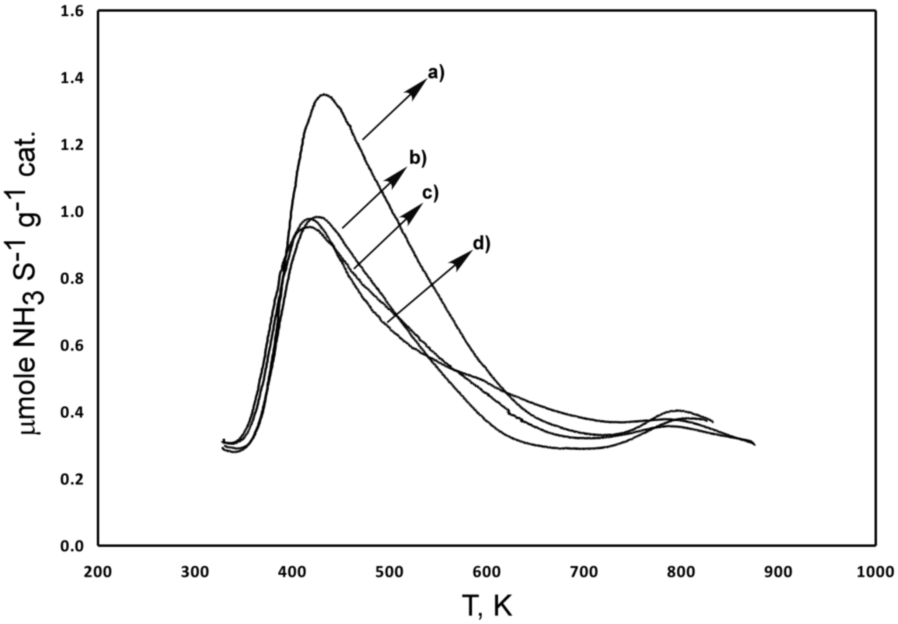

Figure 17: Ammonia Temperature Programmed Desorption (NH_3-TPD) profiles of the sulfide catalysts a) Std. CoMo/γ-Al_2O_3, b) pH4-0.4M_Mo_0.2M_Co, c) pH8.5-0.7M_Mo_0.05M_Co, and d) pH6-0.4M_Mo_0.05M_Co.

4.4 X-Ray Photoelectron Spectroscopy (XPS):

The following sequence of spectra was recorded: survey spectrum of C 1s, O 1s, Al 2p, Mo 3d, Co 2p and C 1s again to check the stability of charge compensation as a function of time and the absence of degradation of the sample during the analyses. For the Mo 3d peak, the energy separation for the doublet was fixed at 3.15 eV. Here, we are focusing solely on the Co 2p and Mo 3d peaks as depicted in Figures 17-24 due to its importance for the catalyst activity. The Mo-3d signals around 232.5 eV and 228.2 eV are those of the MoS_2 phase. While the Co-2p signals at 794.7 eV is due to metallic Co. It's noticed that the sample prepared using polyelectrolytes and loaded with Mo at pH 6 exhibited the larger content of metallic cobalt, which is the cobalt species that is promoting the MoS_2 and is not a cobalt sulfide species. As seen in the edge-rime model, promoting Co species are the ones decorating edges of the layered MoS_2 crystal depicted by the TEM image shown in Figure 25, while the other cobalt species will be converted into an inactive cobalt sulfide phase.

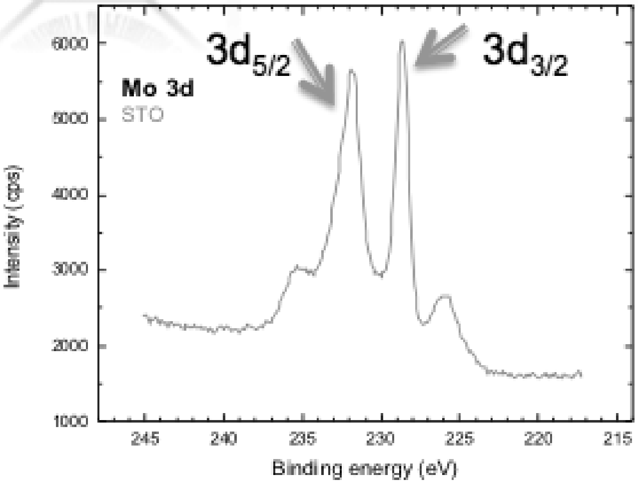

Figure 18: Powder XPS pattern of Mo standard.

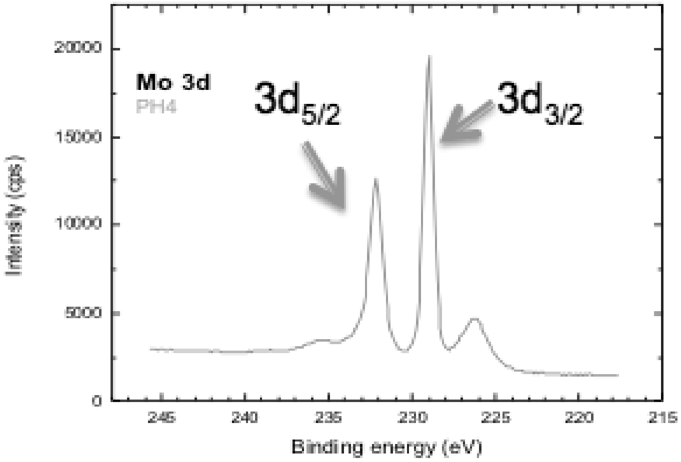

Figure 19: Powder XPS pattern for Mo at pH 4.

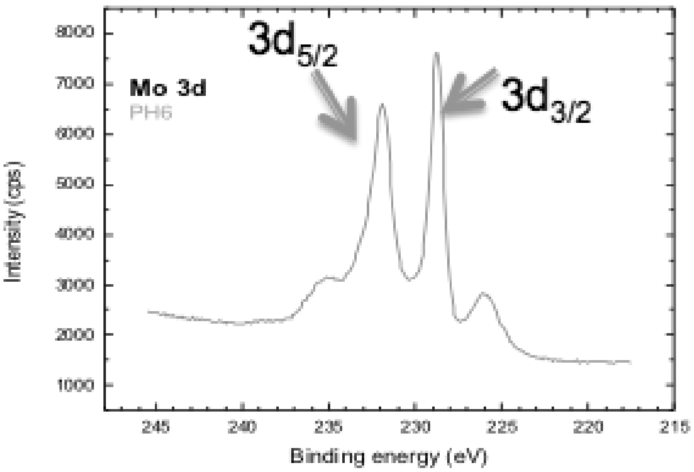

Figure 20: Powder XPS pattern for Mo at pH 6.

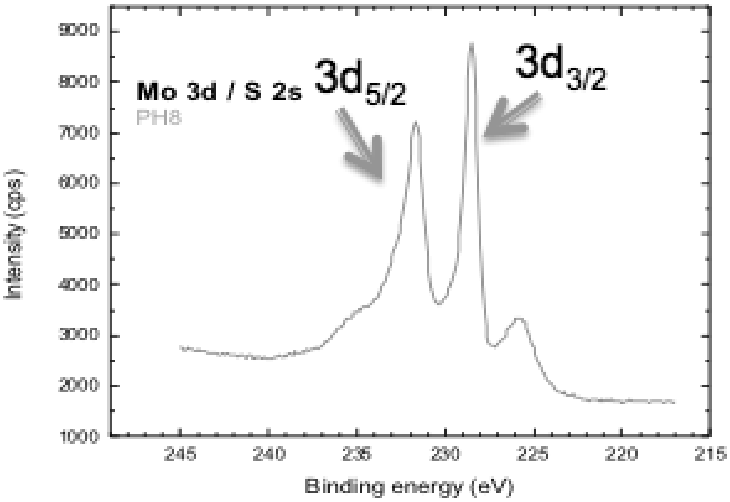

Figure 21: Powder XPS pattern for Mo at pH 8.

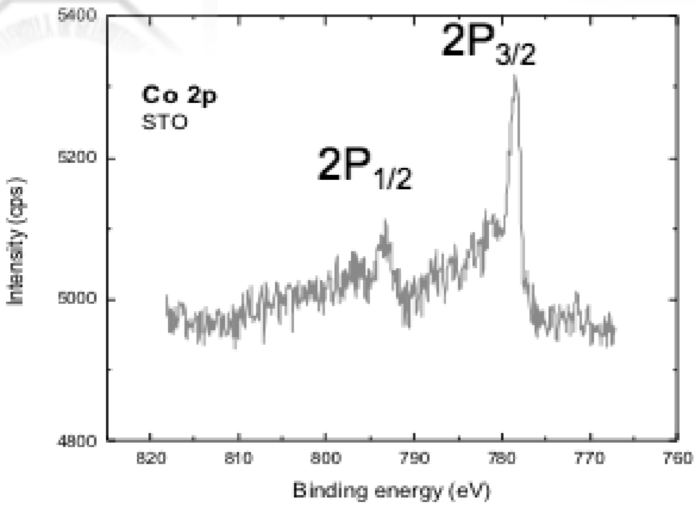

Figure 22: Powder XPS pattern for Co standard.

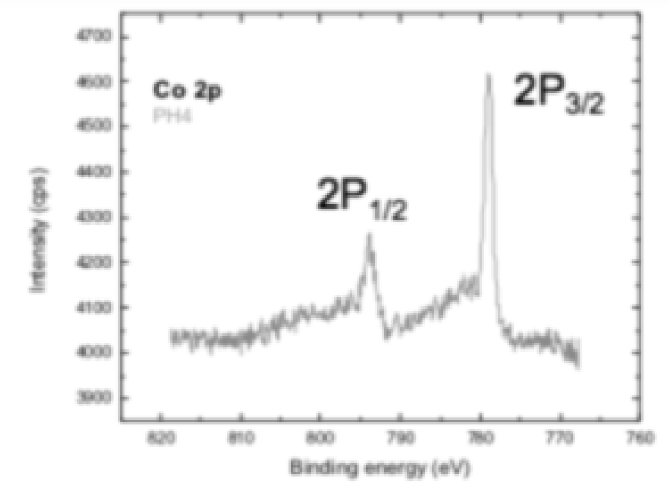

Figure 23:Powder XPS pattern for Co at pH 4.

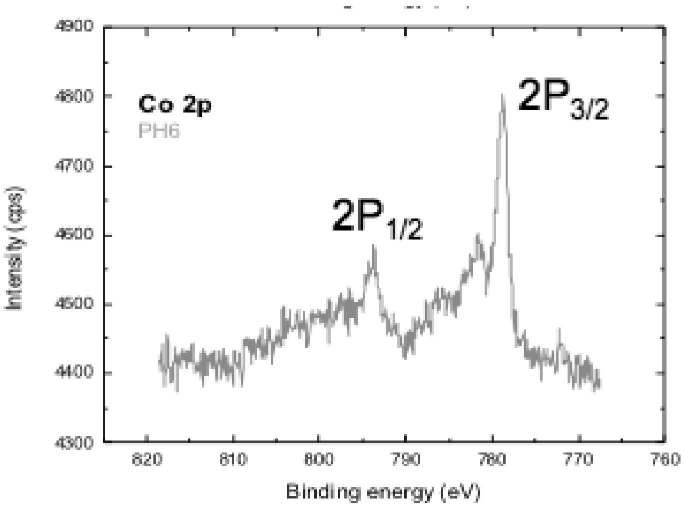

Figure 24: Powder XPS pattern for Co at pH 6.

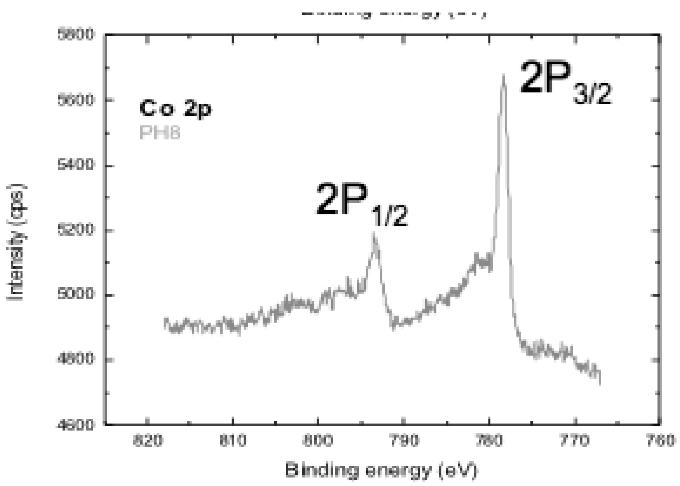

Figure 25: Powder XPS pattern for Co at pH 8.

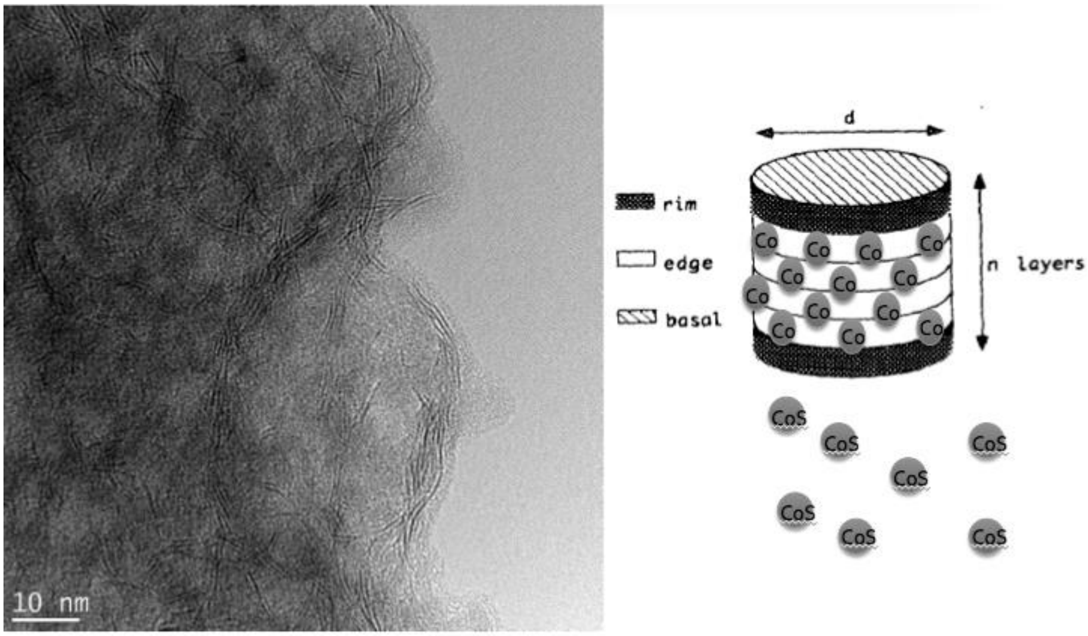

Figure 26: TEM image of Co/MoS_2 catalyst.

4.5 Catalytic Hydrodesulfurization Reaction of Model FCC Gasoline:

The reaction parameters used were as follows:

- Reaction Temperature = 498 k
- Hydrogen pressure = 20 bar
- H_2/HC feed = 200 l/l
- Catalyst mass = 0.5 g
- WHSV = 3 h^{-1}

The reaction was performed for a total of nine hours and the products were sampled every 30 minutes interval. Figure 26 depicts the rate of conversion of 2-MT as a function of time on stream over the selected catalysts. It's noticed that the rate of 2-MT conversion decreases with time over the conventionally made CoMo/Al_2O_3 catalyst, while the 2-MT conversion reaction is relatively higher and more stable over the catalysts prepared using the polyelectrolyte loading method. The higher conversion could be attributed to improved promotion effect of the cobalt on the polyelectrolyte-based system. On the other hand, the stability behavior could be attributed to the relatively stronger and greater density of acid sites found on the conventionally prepared CoMo/Al_2O_3 catalyst that is responsible for deactivating the catalyst by coke formation. Whereas over the catalysts prepared by electrolyte loading method, deactivation by coke formation was slower due to the fact that these catalysts possessed weaker and lesser amounts of acid sites. Similar behavior was observed for the hydrogenation reaction of 2,3-dimethyl-2-butene as shown in figure 27.

Hence, it can be said that the stability of the catalysts prepared by the polyelectrolyte method are attributed to the reduction in the number and strength of acid sites responsible for the catalysts deactivation and this reduction in acidity was achieved by poisoning of the strong acid sites with the carbonaceous materials that are remnant of the coated polymers during the catalyst activation procedure.

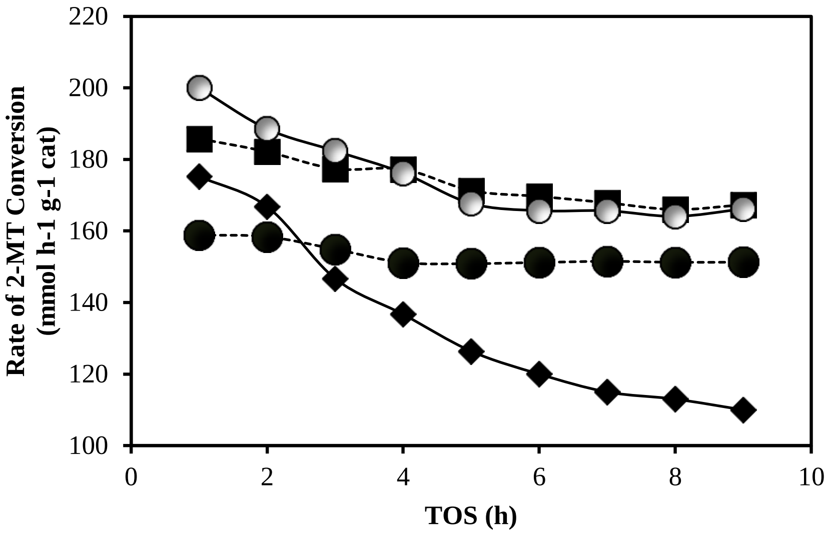

Figure 27: Conversion of 2-MT for Co/Mo/Al_2O_3 standard (◆), pH = 4 (■), pH = 6 (●), pH = 8 (○).

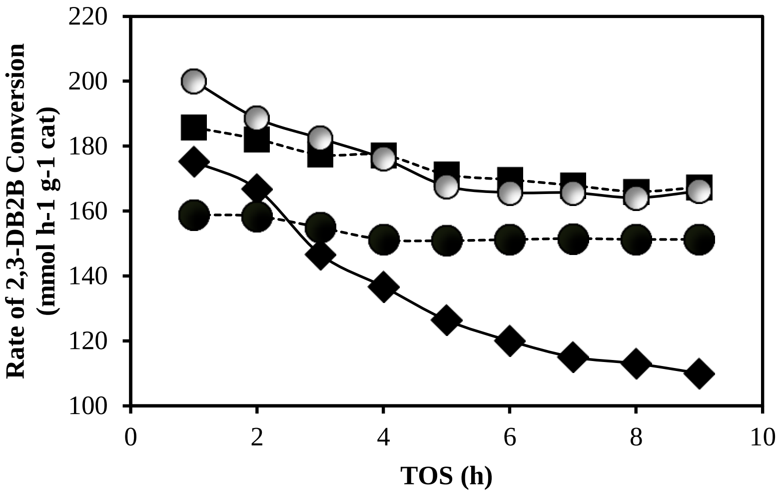

Figure 28: Conversion of 2,3-DB2B for Co/Mo/Al$_2$O$_3$ standard (◆), pH = 4 (■), pH = 6 (●), pH = 8 (○).

CHAPTER 5

CONCLUSION AND FUTURE WORK

5.1 Conclusion:

Upon going through the literature, it was clear that the role of catalyst is crucial for most synthetic and industrial applications. Moreover, several research publications appear annually on HDS technologies. In addition, different modifications in molybdenum catalysts open new possibilities for research and development. Hence, we were able to:

1. Synthesize high loading of about 16% Mo on γ-Al_2O_3.
2. Find that the speciation of molybdenum loaded onto the support is dependent on pH of the solution but not dependent on the concentration of the Mo ions.
3. Understand that increasing positive polyelectrolyte with the use of Mo precursor solution at pH 8 will be the favor the way to obtain high loading of both Mo and Co.

Also, the evaluation of all molybdenum sulfide cobalt promoted ($CoMoS_2$) on gamma alumina (γ-Al_2O_3) catalysts at different pH in the hydrodesulfurization and hydrogenation of synthetic model FCC gasoline was performed. Hence, the synthesized catalysts showed a reasonable activity and improved stability towards HDS and minimized the olefin hydrogenation compared to the standard catalyst prepared in home.

5.2 Future Work and Recommendation:

A few recommendations will be illustrated here concerning the improvement of the catalysts and prospective applications for other reactions. Future work on these catalysts may include the following:

1. Incorporation of different promoter: conventional hydrodesulfurization catalysts are usually promoted with Ni or Co depending on the desired outcome. Suitably promoted catalysts are known to give better performance than their unpromoted counterparts. The choice of promoter usually depends on the nature of feed and the desired reaction. Promotion of this catalyst with other promoter like Phosphorus or magnesium may improve its direct desulfurization functionalities [42].
2. Synthesis of nano-size support and active sites as opposed to micro-sized support used in this study. This can provide high surface area to the catalysts, which means high activity and performance.
3. Use of the catalyst on more refractory alkyl DBT in the real feed: Hydrodesulfurization of alkyl DBTs are known to favor hydrogenation pathway. Since this catalyst show stronger preference for direct desulfurization than hydrogenation, it may prove effective in the HDS of sterically hindered sulfur compounds.
4. The reusability of these catalysts: Our investigations as discussed above show evidence of the active metal deposited majorly in the pores of the polyelectrolyte-coated alumina. This means that reusability of these catalysts

may be enhanced as the active metal are not easily leached inside the pores after several reaction runs.

5. More TEM Micrographs: Future studies should also include clear transmission electron microscopy images in order to ascertain correctly the size of the particles, their stacking height and the distribution.

References

[1] Babich, I.V., & Moulijn, J.A. (2003). *Fuel.* 82, 617.

[2] Song, C. (2003). *Catal. Today.* 86, 211.

[3] Sajkowski, D.J., & Oyama, S.T. (1996). *Appl. Catal. A* 134, 339.

[4] Oyama, S.T. (2003). *J. Catal*. 216, 343.

[5] Whitehurst, D.D., Isoda, T., & Mochida, I. (1998). *Adv. Catal.* 42, 345.

[6] Meijburg, G. (2001). Catalyst Courier No. 46, Akzo Noble.

[7] Olsen, C., Krenzke, L.D., & Watkins, B. (2002). *Proceedings of the 5th International Conference on Refinery Processing, AIChE 2002 Spring National Meeting*, p. 305. New Orleans, LA.

[8] Aridi, T. N., & Al-Daous, M. (2009). *Appl. Catal. A*. 359, 180-187

[9] Rhodes, K.H., Davis, S.A., Caruso, F., Zhang, B., & Mann, S., (2000). *Chem. Mater*, 12, 2832-2834.

[10] Pincus, P. (1991). *Macromolecules.* 24, 2912.

[11] Afanasiev, P., Xia, G.-F., Berhault, G., Jouguct, B., & Lacroix, M. (1999b). *Chem.*

[12] Rueda, N., Bacaud, R., & Varinat, M. (1997). *J. Catal.* 169, 404

[13] Topsoe, H., & Clausen, B.S. (1981). *Catal. Rev.-Sci. Eng*. 22, 401

[14] Carrier, X., Lambert, J.F., & Che, M. (1997). *J. Am. Chem. Soc.* 119, 10137

[15] Breysse, M., Afanasiev, P., Geantet, C., & Varinat, M. (2003). *Catal. Today* 86, 5

[16] R.R. Bharvani, R.S. Henderson, *Hydrocarb. Process*. 81, (2002) 61–64.

[17] A. Stanislaus, A. Marafi, M. S. Rana,, *Catalysis Today* 153, (2010) 1-68.

[18] T. Fujikawa, H. Kimura, K. Kiriyama, K. Hagiwara, *Catal. Today*, (2006) 188–193.

[19] (a) NEBuLA-20 (introduced in market 2004): http://www.albemarle.com/TDS/HPC/NEBULA-20 The%20 next step into deep space.pdf; (b) Y. Gochi, C. Ornelas, F. Paraguay, S. Fuentes, L. Alvarez, J.L. Rico, G. Alonso-Nunez, Catal. Today 107–108 (2005) 531–536.

[20] D. Krenzke, M. Zehender, (2002)., *Hydrocarbon Asia*, 12, 44–48.

[21] Topsoe hydrotreating catalysts: http://www.topsoe.com/products/CatalystPortfolio.aspx.

[22] Goula, M.A., Kordulis, C., & Lycourghiotis, A. (1992). *J. Catal*. 133, 486.

[23] Bezverkhyy, I., Afanasiev, P., & Lacroix, M. (2005). *J. Catal*. 230, 133.

[24] Lee, J.J., Kim, H., & Moon, S.H. (2003). *Appl. Catal. B* 41, 171

[25] Mauge, F., Vallet, A., Bachelier, J., Duchet, J.C., & Lavalley, J.C. (1996). *J. Catal.* 162, 88.

[26] Okamoto, Y., & Kubota, T. (2003). *Catal. Today* 86, 31.

[27] Murase, K., Ando, H., Matsubara, E., Hirato, T., & Awakura, Y. (2000). *J. Electrochem. Soc*. 147(6), 2210.

[28] Jolivet, J.P. (2000). Metal Oxide Chemistry and Synthesis: From Solution to Solid State. *Wiley, West Sussex*.

[29] Topsoe, H., Clausen, B.S., & Massoth, F.E. (1996). Hydrotreating Catslysis Science and Technology,. In (*Anderson, J.R., & Boudart, M., Eds.),* Vol. 11, pp. 65-69. Springer, New York.

[30] Candia, R., Sorensen, O., Villadsen, J., Topsoe, N., Clausen, B.S., & Topsoe, H. (1984). *Bull. Soc. Chim. Belg*. 93, 763.

[31] Bouwens, S.M.A.M., van Zon, F.B.M., van Dijk, M.P., van der Kraan, A.M., de Beer, V.H.J., van Veen, J.A.R., & Koningsberger, D.C. (1994). *J. Catal.* 146, 375.

[32] Zhao, E., Hardcastle, S.E., Pacheco, G., Garcia, A., Blumenfeld, A.L., & Fripiat, J.J. (1999). *Micropor. Mesopor. Mater*. 31, 9.

[33] Ma, X., Sakanishi, K., & Mochida, I. (1994). *Ind. Eng. Chem. Res.* 33, 218.

[34] Meille, V., Schulz, E., Lemaire, M., & Vrinat, M. (1997). *J. Catal.* 170, 29.

[35] Michaud, P., Lemberton, J.L., & Perot, G. (1998). *Appl. Catal. A* 169, 343.

[36] Shafi, R., & Hutchings, G.J. (2000). *Catal. Today* 59, 423.

[37] Bej, S.K., Maity, S.K., & Turaga, U.T. (2004). *Energy Fuels* 18(5), 1227.

[38] Lamure-Meille, V., Schulz, E., Lemaire, M., & Vrinat, M. (1995). *Appl. Catal. A.* 131, 143.

[39] Sanchez-Delgado, R.A. (1994). *J. Mol. Catal*. 86, 287.

[40] Perot, G. (2003). *Catal. Today* 86, 11.

[41] K. Sing, D. Evertt, R. Haul, L. Moscou, R. Pierotti, J. Rouquerol, T. Siemieiewaska, *Pure. Appl. Chem.,* 57 (1985) 603.

VITAE

NAME: Noktan Mohammed Noktan AlYami

NATIONALITY: Saudi

DATE OF BIRTH: 21-03-1987

EMAIL: yaminm0l@aramco.com

EDUCATION: June, 2009B.S. in Industrial Chemistry from King Fahd University of Petroleum & Minerals

May 2013, MS in Chemistry from King Fahd University of Petroleum & Minerals